

## Slow hot carrier cooling in cesium lead iodide perovskites

Qing Shen, Teresa S. Ripolles, Jacky Even, Yuhei Ogomi, Koji Nishinaka, Takuya Izuishi, Naoki Nakazawa, Yaohong Zhang, Chao Ding, Feng Liu, Taro Toyoda, Kenji Yoshino, Takashi Minemoto, Kenji Katayama, and Shuzi Hayase

Citation: *Appl. Phys. Lett.* **111**, 153903 (2017);

View online: <https://doi.org/10.1063/1.4991993>

View Table of Contents: <http://aip.scitation.org/toc/apl/111/15>

Published by the [American Institute of Physics](#)

---

### Articles you may be interested in

[Spectroscopic studies of chiral perovskite nanocrystals](#)

*Applied Physics Letters* **111**, 151102 (2017); 10.1063/1.5001151

[Intrinsic point defects in inorganic perovskite CsPbI<sub>3</sub> from first-principles prediction](#)

*Applied Physics Letters* **111**, 162106 (2017); 10.1063/1.5001535

[Unusual defect physics in CH<sub>3</sub>NH<sub>3</sub>PbI<sub>3</sub> perovskite solar cell absorber](#)

*Applied Physics Letters* **104**, 063903 (2014); 10.1063/1.4864778

[Synthesis of Cs<sub>2</sub>AgSbCl<sub>6</sub> and improved optoelectronic properties of Cs<sub>2</sub>AgSbCl<sub>6</sub>/TiO<sub>2</sub> heterostructure driven by the interface effect for lead-free double perovskites solar cells](#)

*Applied Physics Letters* **111**, 151602 (2017); 10.1063/1.4999192

[Irreversible light-soaking effect of perovskite solar cells caused by light-induced oxygen vacancies in titanium oxide](#)

*Applied Physics Letters* **111**, 153501 (2017); 10.1063/1.4994085

[Perspective: Theory and simulation of hybrid halide perovskites](#)

*The Journal of Chemical Physics* **146**, 220901 (2017); 10.1063/1.4984964

---

**Scilight**

Sharp, quick summaries **illuminating**  
the latest physics research

Sign up for **FREE!**



## Slow hot carrier cooling in cesium lead iodide perovskites

Qing Shen,<sup>1,a)</sup> Teresa S. Ripolles,<sup>2,a)</sup> Jacky Even,<sup>3,a)</sup> Yuhei Ogomi,<sup>2</sup> Koji Nishinaka,<sup>2</sup> Takuya Izuishi,<sup>1</sup> Naoki Nakazawa,<sup>1</sup> Yaohong Zhang,<sup>1</sup> Chao Ding,<sup>1</sup> Feng Liu,<sup>1</sup> Taro Toyoda,<sup>1</sup> Kenji Yoshino,<sup>4</sup> Takashi Minemoto,<sup>5</sup> Kenji Katayama,<sup>6</sup> and Shuzi Hayase<sup>2,a)</sup>

<sup>1</sup>Department of Engineering Science, Faculty of Informatics and Engineering, The University of Electro-Communications, 1-5-1 Chofugaoka, Chofu, Tokyo 182-8585, Japan

<sup>2</sup>Graduate School of Life Science and Systems Engineering, Kyushu Institute of Technology, 2-4 Hibikino, Wakamatsu, Kitakyushu 808-0196, Japan

<sup>3</sup>Fonctions Optiques pour les Technologies de l'information, UMR 6082, INSA, 35708 Rennes, France

<sup>4</sup>Department of Electrical and Electronic Engineering, Miyazaki University, 1-1 Gakuen, Kibanadai-nishi, Miyazaki 889-2192, Japan

<sup>5</sup>Department of Electrical and Electronic Engineering, Faculty of Science and Engineering, Ritsumeikan University, 1-1-1 Nojihigashi, Kusatsu, Shiga 525-8577, Japan

<sup>6</sup>Department of Applied Chemistry, Faculty of Science and Engineering, Chuo University, 1-13-27 Kasuga, Bunkyo, Tokyo 112-8551, Japan

(Received 25 June 2017; accepted 25 September 2017; published online 11 October 2017)

Lead halide perovskites are attracting a great deal of interest for optoelectronic applications such as solar cells, LEDs, and lasers because of their unique properties. In solar cells, heat dissipation by hot carriers results in a major energy loss channel responsible for the Shockley–Queisser efficiency limit. Hot carrier solar cells offer the possibility to overcome this limit and achieve energy conversion efficiency as high as 66% by extracting hot carriers. Therefore, fundamental studies on hot carrier relaxation dynamics in lead halide perovskites are important. Here, we elucidated the hot carrier cooling dynamics in all-inorganic cesium lead iodide (CsPbI<sub>3</sub>) perovskite using transient absorption spectroscopy. We observe that the hot carrier cooling rate in CsPbI<sub>3</sub> decreases as the fluence of the pump light increases and the cooling is as slow as a few 10 ps when the photoexcited carrier density is  $7 \times 10^{18} \text{ cm}^{-3}$ , which is attributed to phonon bottleneck for high photoexcited carrier densities. Our findings suggest that CsPbI<sub>3</sub> has a potential for hot carrier solar cell applications.

Published by AIP Publishing. <https://doi.org/10.1063/1.4991993>

Organic-inorganic hybrid perovskite solar cells have been evolving rapidly over the past five years, and the record power conversion efficiency (PCE) has reached over 22%.<sup>1–22</sup> Organolead halide perovskites in the form of AMX<sub>3</sub> (A = organic molecule, e.g., CH<sub>3</sub>NH<sub>3</sub> (MA), M = Pb, X = Cl, Br, and I) can be simply crystallized from solution at low temperatures ( $\leq 100^\circ\text{C}$ ). Thus, perovskite materials can be utilized as light absorbers in solar cells. In particular, MAPbI<sub>3</sub> has some unique properties which are attractive for photovoltaic applications, mainly: (1) a high optical absorption coefficient;<sup>23,24</sup> (2) small exciton binding energy (about 20 meV);<sup>25</sup> (3) long photoexcited carrier lifetimes ( $> 100$  ns) and long diffusion lengths (100–1000 nm or even longer);<sup>26,27</sup> and (4) no deep state defects and very small Urbach energy (15 meV).<sup>28</sup> To further improve the photovoltaic properties, it is very important to understand photoexcited carrier dynamics, charge separation, and recombination mechanisms at each interface in the device. Meanwhile, some critical issues for perovskite solar cells include improving the material stability and understanding the degradation mechanisms. Recently, all-inorganic cesium lead halide (CsPbX<sub>3</sub>) perovskite solar cells show the potential for making stable photovoltaic devices, even more stable than the

standard MAPbI<sub>3</sub> solar cells,<sup>29–34</sup> and phase stabilization can be reached in CsPbI<sub>3</sub> quantum dot based solar cells.<sup>35</sup>

For future applications, such as hot carrier solar cells<sup>36</sup> and electrically pumped lasers,<sup>37,38</sup> an understanding of the ultrafast photoexcited carrier dynamics is crucial, especially hot carrier cooling. Price and co-workers have recently reported on the hot-carrier cooling dynamics in MAPbI<sub>3</sub> by using transient absorption (TA) spectroscopy.<sup>39</sup> The authors observed that a quasi-thermalized carrier distribution was created within 100 fs in MAPbI<sub>3</sub>, and the hot carriers cooled with a decay constant of a few 100 fs within the first 2 ps and then a slower one after 2 ps. This behavior was attributed to an average of hot electron and hole distributions. The influence of electron-phonon interactions was stressed and a phonon bottleneck was described, but the effect of organic cations remained an open question. Very recently, Yang and co-workers also studied the hot carrier cooling dynamics in MAPbI<sub>3</sub> using the TA technique, which was attributed to a hot phonon bottleneck related to a non-equilibrium LO-phonon distribution. The hot carrier cooling was slowed down by three to four orders of magnitude in time above a critical injection carrier density of  $\sim 5 \times 10^{17} \text{ cm}^{-3}$ .<sup>40</sup> On the other hand, Yamashita and co-workers calculated the hot-carrier lifetimes from electron–phonon interactions in CsPbI<sub>3</sub> using first principles calculations.<sup>41</sup> Their results show that holes in CsPbI<sub>3</sub> have very long lifetimes in the region situated 0.6 eV below the top of the valence band. They proposed that the slow hot hole cooling process may result from the

<sup>a)</sup>Authors to whom correspondence should be addressed: shen@pc.uec.ac.jp; teresa@life.kyutech.ac.jp; jacky.even@insa-rennes.fr; and hayase@life.kyutech.ac.jp

smaller number of relaxation paths due to the low density of states in the valence band in CsPbI<sub>3</sub>,<sup>41</sup> although similar electron-phonon and hole-phonon processes, namely, acoustic deformation and LO Fröhlich processes, are predicted from symmetry considerations. This is in sharp contrast to classical semiconductors.<sup>42,43</sup> Very recently, Chung and co-workers studied hot carrier relaxation dynamics in CsPbBr<sub>3</sub> and CsPbI<sub>3</sub> perovskite nanocrystals using the TA technique, and ultrafast (<0.6 ps) hot carrier relaxation dynamics were observed.<sup>44</sup>

In this study, we investigate hot carrier relaxation dynamics in the bulk CsPbI<sub>3</sub> film using the TA technique. We show the sign of a non-thermalized carrier distribution in CsPbI<sub>3</sub> after ultrashort light pulse excitation. We observe that the hot carrier cooling rate in CsPbI<sub>3</sub> decreases as the fluence of the pump light increases and the cooling is as slow as a few 10 ps when the photoexcited carrier density is  $7 \times 10^{18} \text{ cm}^{-3}$ , which is attributed to the hot phonon bottleneck effect similar to the previous studies for bulk MAPbI<sub>3</sub> and FAPbI<sub>3</sub>.<sup>39,40</sup>

Immediately after excitation by a pump pulse with photon energy larger than the bandgap energy, electrons and holes are excited to higher excited states. Then, after the duration of the pulsed pump light irradiation, the photoexcited carriers begin to relax and lose their excess energy towards equilibrium through (1) carrier-carrier collisions and (2) phonon emission.<sup>45</sup> During the stage (1), carrier-carrier collisions result in a uniform distribution of the photocarriers that can be described by the Boltzmann distribution with a much higher temperature than the lattice temperature, and these carriers are called “hot” carriers. This is the “initial thermalization” of photocarriers, and there is no energy lost.<sup>45</sup> During stage (2), hot carriers lose energy to the lattice through the emission of phonons. As a result, the total energy and the temperature of the carriers decrease with the phonon emission. Eventually, the carriers cool down and their temperature is the same as that of the lattice. This is the “hot carrier cooling” process.<sup>45</sup> In this study, we focus especially on hot carrier cooling process in the inorganic halide perovskite CsPbI<sub>3</sub>, which can be monitored using time-resolved TA spectra.

The CsPbI<sub>3</sub> samples were prepared on mesoporous Al<sub>2</sub>O<sub>3</sub> layers using the method reported previously.<sup>29</sup> The details are described in the [supplementary material](#). In order to keep the crystal phase of the CsPbI<sub>3</sub> perovskite film stable, some considerations in the experimental procedure were carried out. Before the perovskite deposition on the top of the mesoporous Al<sub>2</sub>O<sub>3</sub> film, a plasma treatment was performed. Then, the CsPbI<sub>3</sub> synthesis was done in the glove box under the nitrogen environment to avoid any contact with oxygen or moisture. Finally, before removing substrates from the glove box, a thin film of a polymer poly(methyl methacrylate), i.e., PMMA, was deposited by a spin coater in order to encapsulate the absorber film. The crystal structure of the CsPbI<sub>3</sub> was confirmed to be cubic phase by X-Ray Diffraction (XRD) characterization as shown in Fig. 1(a). Figure S1 ([supplementary material](#)) shows the XRD patterns of the sample measured soon after the preparation and 2h after the preparation, which confirm that the phase transition of the CsPbI<sub>3</sub> samples did not occur. The thickness was

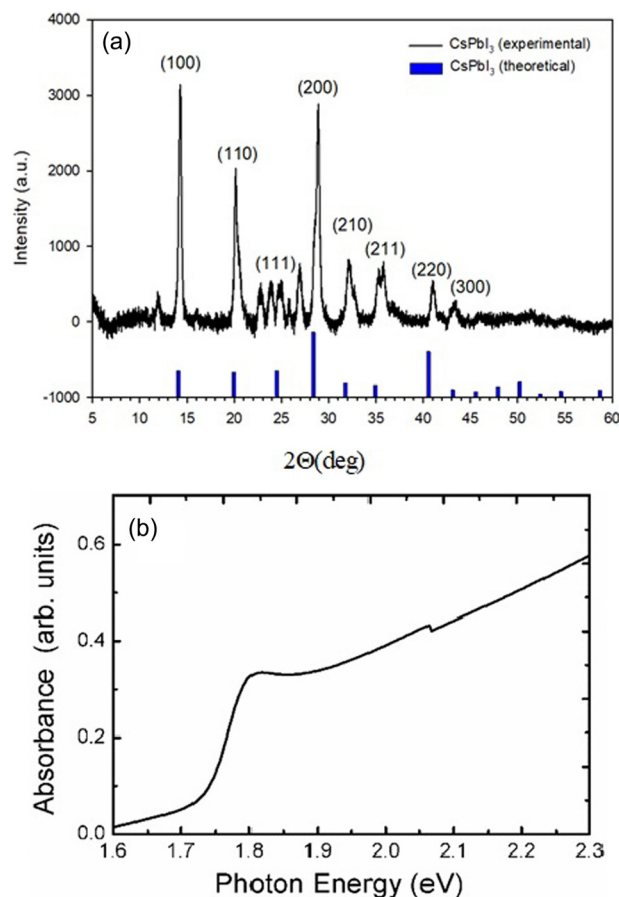


FIG. 1. (a) XRD pattern and (b) typical optical absorption spectrum of CsPbI<sub>3</sub>.

measured to be about 300 nm by using a vertical resolution non-contact surface profiler with the technique of white light interferometric microscopy. From the SEM image of the sample surface as shown in Fig. S2 ([supplementary material](#)), it is observed that the CsPbI<sub>3</sub> is a continuous film. Figure 1(b) shows a typical optical absorption spectrum of the CsPbI<sub>3</sub> samples. A clear optical absorption peak can be observed at 1.8 eV, corresponding to the excitonic transitions.<sup>40</sup>

Figures 2(a) and 2(b) show the TA spectra and the normalized ones of CsPbI<sub>3</sub>/Al<sub>2</sub>O<sub>3</sub> for delay times ranging from 0.1 ps to 6.4 ps, respectively, where the pump light wavelength is 470 nm and its photon energy is 2.6 eV. It was found that the TA spectra became very different and complicated if the CsPbI<sub>3</sub> was unstable and had a phase transition, of which an example is shown in Fig. S3 in the [supplementary material](#). So, the beautiful TA spectra as shown in Fig. 2 confirm that the crystal phase was stable during the TA measurements. There is no electron or hole transfer from CsPbI<sub>3</sub> to Al<sub>2</sub>O<sub>3</sub>; therefore, hot carrier relaxation dynamics in CsPbI<sub>3</sub> can be studied without considering any effect of charge transfer. As shown in Fig. 2, a bleaching peak at 1.8 eV is observed clearly for all delay times, which corresponds to the optical absorption peak of CsPbI<sub>3</sub> as shown in Fig. 1(b) and is called the “band-edge peak” here. Around 0.1 ps, a broad bleaching peak appears at about 2.0 eV well below the pump light energy (2.6 eV) and is called the “hot carrier peak” here. The appearance of the “hot carrier peak”

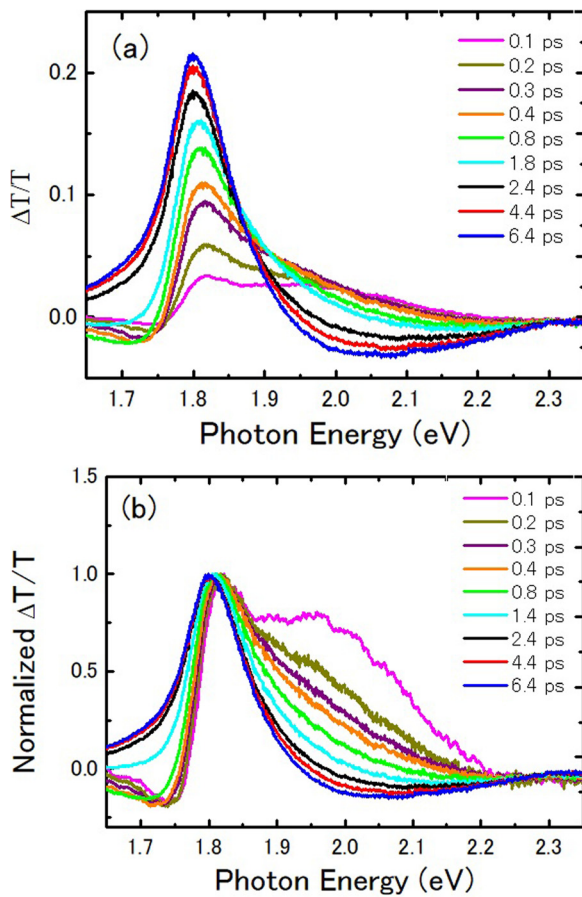


FIG. 2. (a) TA spectra and (b) normalized TA spectra of CsPbI<sub>3</sub>/Al<sub>2</sub>O<sub>3</sub> for times from 0.1 ps to 6.4 ps, respectively. For the TA spectra measurements, the pump light wavelength is 470 nm (pump energy is 2.6 eV) and the photoexcited carrier density is  $1.3 \times 10^{18} \text{ cm}^{-3}$ .

indicates a non-thermal equilibrium hot carrier distribution at the very early time after light excitation. Then, as the delay time increases up to 0.3 ps, the “hot carrier peak” disappears. These changes in the TA spectra versus time reflect a clear out-of-equilibrium redistribution of carriers through many-body carrier-carrier scattering mechanisms, before the creation of thermalized carrier distributions by phonon emission.<sup>45,46</sup> Meanwhile, a negative TA peak appears just below the bandgap (1.75 eV), which is considered to be due to the interplay between bandgap renormalization and the hot-carrier distribution.<sup>39,40</sup> For delay times larger than 0.3 ps, the “hot carrier peak” disappears and the high-energy tail of the spectrum broadens simultaneously (here called the “hot carrier bleach”) as a result of carrier thermalization through carrier-carrier scattering. These results indicate that a quasi-thermal equilibrium of the charge carriers is finally reached at around 0.3 ps after generation, which is the initial thermalization as mentioned above.<sup>47</sup> For times longer than 0.3 ps, the distribution of the carriers, which are in quasi-thermal equilibrium, can be considered to depend only on an effective carrier temperature  $T_C$ . This process corresponds to the hot carrier cooling.  $T_C$  is calculated by fitting the TA spectra above the band edge (between 1.93 eV and 2.1 eV) to a Boltzmann distribution.<sup>39,40</sup> Figure 3(a) shows an example of the fitting result, describing the high energy tail with a Boltzmann distribution. For such calculations, we assume

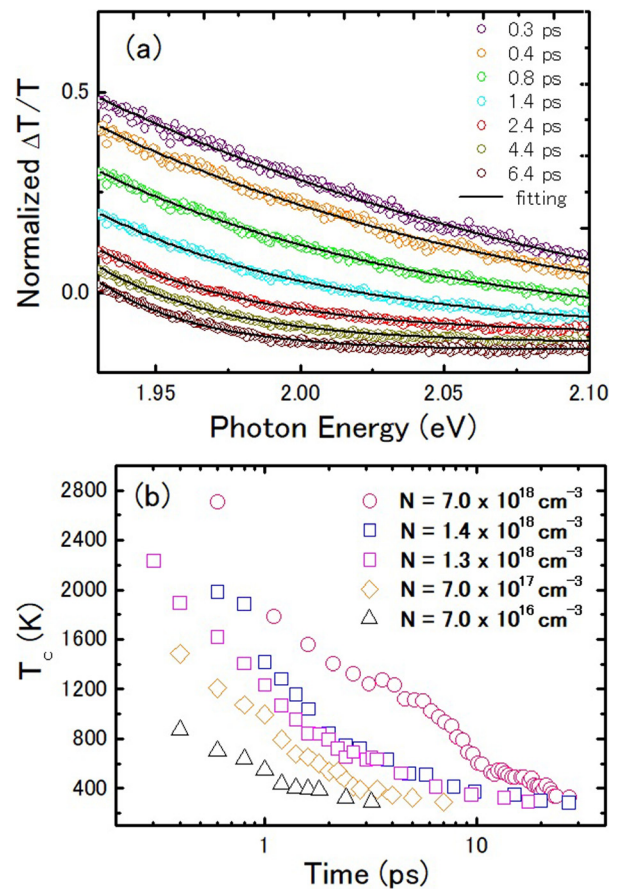


FIG. 3. (a) A global fit of the high-energy tail for each time to a Boltzmann distribution between 1.93 eV and 2.1 eV for CsPbI<sub>3</sub>/Al<sub>2</sub>O<sub>3</sub> with a photoexcited carrier density of  $1.3 \times 10^{18} \text{ cm}^{-3}$ ; (b) the change in  $T_C$  against time for different photoexcited carrier densities from  $7 \times 10^{16} \text{ cm}^{-3}$  to  $7 \times 10^{18} \text{ cm}^{-3}$ .

the following facts: (1) the TA signal is proportional to the change in the absorption coefficient, i.e.,  $\Delta T/T \propto \Delta \alpha$ ; (2) the density of states is approximately constant in the analyzed region, i.e., the high energy tail; and (3) the distribution of the carriers in quasi-thermal equilibrium follows a Boltzmann distribution, i.e.,  $\Delta T/T[E > 1.9 \text{ eV}] \propto e^{-(E-E_f)/(K_B T_C)}$ , where  $E_f$  is the quasi-Fermi energy and  $K_B$  is the Boltzmann constant.<sup>39,40</sup> Figure 3(b) shows the changes in the hot carrier temperature  $T_C$  against time for different photoexcited carrier densities, which were obtained from the fittings to the TA spectra of the same samples obtained at different pump light intensities. It can be clearly observed that the hot carrier cooling depends on the photoexcited carrier density significantly. For low photoexcited carrier density of  $7 \times 10^{16} \text{ cm}^{-3}$ , the cooling of the hot carriers only shows a fast process with a time constant less than 1 ps. When the photoexcited carrier density is larger than  $7 \times 10^{17} \text{ cm}^{-3}$ , another slow cooling process appears and the cooling time to reach room temperature becomes longer and longer as the photoexcited carrier density increases. Specifically, it takes 30 ps to reach room temperature for the photoexcited carrier density of  $7 \times 10^{18} \text{ cm}^{-3}$ . This result indicates the hot-phonon bottleneck in CsPbI<sub>3</sub> perovskite, as also observed by other groups in MAPbI<sub>3</sub> and FAPbI<sub>3</sub> perovskites.<sup>39,40</sup> Figure 4 shows the time resolved TA spectra of the same sample measured with the pump light wavelength

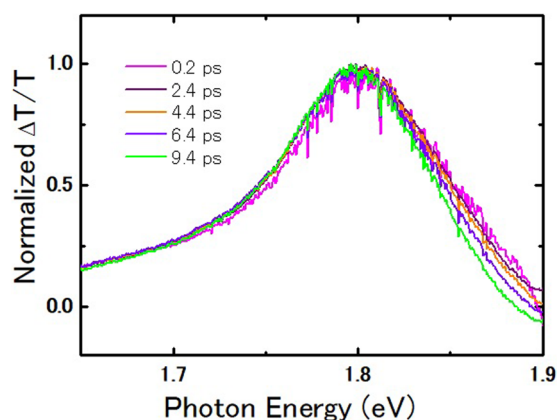


FIG. 4. Normalized TA spectra of CsPbI<sub>3</sub>/Al<sub>2</sub>O<sub>3</sub> for times from 0.2 ps to 9.4 ps. For TA spectra measurements, the pump light wavelength is 650 nm (pump energy is 1.9 eV), and the photoexcited carrier density is  $7 \times 10^{17} \text{ cm}^{-3}$ .

of 650 nm. In this case, the photon energy of the pump light is 1.9 eV, which is only about 0.1 eV larger than the bandgap energy of CsPbI<sub>3</sub>. As a result, there is no obvious broadening in the high energy tail, indicating that almost no hot carriers exist in this case.

Based on the above results, we have observed two processes for hot carrier relaxation from excitation to cooling down to the lattice temperature (i.e., the room temperature) in CsPbI<sub>3</sub> under our experimental conditions. The first process is the initial thermalization. The non-equilibrium distribution of photoexcited carriers was produced initially, and then, an ultrafast out-of equilibrium redistribution of carriers occurs through carrier-carrier scattering to reach a quasi-equilibrium by up to 0.3 ps. In semiconductors, the initial thermalization process related to many-body effects (such as carrier-carrier scattering and carrier-optical phonon scattering) depends strongly on many factors such as carrier density and physical properties of the sample. Typically, the thermalization time was reported to be less than 1–2 ps in the bulk semiconductor.<sup>45,47</sup> So, the thermalization time of 0.3 ps observed in the CsPbI<sub>3</sub> here is thought to be reasonable. This time is a little slower compared to the reported time of 100 fs in MAPbI<sub>3</sub>.<sup>39,40</sup> The reason for this difference will be studied and made clear. The second one is the carrier cooling process. In this process, fast hot carrier cooling occurs on a time scale of sub-ps and slower hot carrier cooling occurs on a time scale from a few ps to a few 10 ps. The fast cooling process is considered to reflect the initial electron-phonon interaction before reaching the hot-phonon condition, and the following slow cooling process is due to the hot phonon bottleneck effect.<sup>39</sup> Similar fast hot carrier cooling processes have been observed for MAPbI<sub>3</sub> (Refs. 39 and 40) for different excitation intensities. However, the slow hot carrier cooling process can only be observed under the condition of high excitation intensity where the hot-phonon distributions can be created.<sup>40</sup> These findings indicate that inorganic cation Cs in the perovskite seems to have a similar effect on hot carrier cooling as the organic ions (MA or FA) reported in Refs. 39 and 40. The hot carrier cooling dynamics observed in the bulk CsPbI<sub>3</sub> film in this study is quite slower compared to those observed in the CsPbI<sub>3</sub> nanocrystals.<sup>44</sup> This result

suggests that there may be some intrinsic difference in the hot carrier relaxation processes between the bulk CsPbI<sub>3</sub> and the CsPbI<sub>3</sub> nanocrystals. A possible explanation may rely on subtle structural differences. Polymorphism indeed affects the cubic black phase of CsPbI<sub>3</sub>, leading to slightly distorted black phases different from the yellow phase.<sup>48</sup> The competition between these polymorphs and the yellow phase may result from the strong phonon anharmonicity predicted for the cubic phase and the structural instabilities at various points of the Brillouin zone.<sup>49</sup> It is also known from the exciton fine structure that polymorphism affects in a similar way CsPbBr<sub>3</sub> nanocrystals depending on the size and the growth procedure.<sup>50</sup> However, other explanations related to the role of surface states in nanocrystals cannot be ruled out and are difficult to infer from the present results on thin films.

In conclusion, we elucidated the hot carrier cooling dynamics in the CsPbI<sub>3</sub> perovskite. We find that a non-thermalized carrier population is created within a few 100 fs after excitation. Hot carriers cool slowly to reach the room temperature in a few 10 ps for higher photoexcited carrier density, which originates from a bottleneck of the carrier-phonon interactions. Our findings shed light on the potential application of CsPbI<sub>3</sub> to hot carrier solar cells.

See [supplementary material](#) for experimental methods, XRD patterns of the CsPbI<sub>3</sub> perovskite measured soon after preparation and 2 h after preparation, SEM images of the sample surface, as well as TA spectra of the CsPbI<sub>3</sub> perovskite after phase transition.

This work was supported by the CREST program of Japan Science and Technology Agency (JST). The authors thank Ye Yang greatly for his very helpful discussions on the experimental results. This work was also supported by JSPS KAKENHI Grant No. JP16K17947.

<sup>1</sup>W. S. Yang, B.-W. Park, E. H. Jung, N. J. Jeon, Y. C. Kim, D. U. Lee, S. S. Shin, J. Seo, E. K. Kim, J. H. Noh, and S. I. Seok, *Science* **356**, 1376 (2017).

<sup>2</sup>H. S. Jung and N. G. Park, *Small* **11**, 10 (2015).

<sup>3</sup>M. A. Green, A. Ho-Baillie, and H. J. Snaith, *Nat. Photonics* **8**, 506 (2014).

<sup>4</sup>N. J. Jeon, J. H. Noh, Y. C. Kim, W. S. Yang, S. Ryu, and S. Seok, *Nat. Mater.* **13**, 897 (2014).

<sup>5</sup>M. Z. Liu, M. B. Johnston, and H. J. Snaith, *Nature* **501**, 395 (2013).

<sup>6</sup>H. P. Zhou, Q. Chen, G. Li, S. Luo, T. B. Song, H. S. Duan, Z. R. Hong, J. B. You, Y. S. Liu, and Y. Yang, *Science* **345**, 542 (2014).

<sup>7</sup>J. Burschka, N. Pellet, S. J. Moon, R. Humphry-Baker, P. Gao, M. K. Nazeeruddin, and M. Gratzel, *Nature* **499**, 316 (2013).

<sup>8</sup>G. E. Eperon, V. M. Burlakov, A. Goriely, and H. J. Snaith, *ACS Nano* **8**, 591 (2014).

<sup>9</sup>J. H. Im, J. Chung, S. J. Kim, and N. G. Park, *Nanoscale Res. Lett.* **7**, 353 (2012).

<sup>10</sup>H. S. Kim, C. R. Lee, J. H. Im, K. B. Lee, T. Moehl, A. Marchioro, S. J. Moon, R. Humphry-Baker, J. H. Yum, J. E. Moser, M. Gratzel, and N. G. Park, *Sci. Rep.* **2**, 591 (2012).

<sup>11</sup>M. M. Lee, J. Teuscher, T. Miyasaka, T. N. Murakami, and H. J. Snaith, *Science* **338**, 643 (2012).

<sup>12</sup>V. Gonzalez-Pedro, E. J. Juarez-Perez, W.-S. Arsyad, E. M. Barea, F. Fabregat-Santiago, I. Mora-Sero, and J. Bisquert, *Nano Lett.* **14**, 888 (2014).

<sup>13</sup>J. H. Noh, S. H. Im, J. H. Heo, T. N. Mandal, and S. I. Seok, *Nano Lett.* **13**, 1764 (2013).

<sup>14</sup>N. G. Park, *J. Phys. Chem. Lett.* **4**, 2423 (2013).

- <sup>15</sup>J. T.-W. Wang, J. M. Ball, E. M. Barea, A. Abate, J. A. Alexander-Webber, J. Huang, M. Saliba, I. Mora-Sero, J. Bisquert, H. J. Snaith, and R. J. Nicholas, *Nano Lett.* **14**, 724 (2014).
- <sup>16</sup>A. Abate, M. Saliba, D. J. Hollman, S. D. Stranks, K. Wojciechowski, R. Avolio, G. Grancini, A. Petrozza, and H. J. Snaith, *Nano Lett.* **14**, 3247 (2014).
- <sup>17</sup>A. Amat, E. Mosconi, E. Ronca, C. Quarti, P. Umari, M. K. Nazeeruddin, M. Grätzel, and F. De Angelis, *Nano Lett.* **14**, 3608 (2014).
- <sup>18</sup>Q. Chen, H. Zhou, T.-B. Song, S. Luo, Z. Hong, H.-S. Duan, L. Dou, Y. Liu, and Y. Yang, *Nano Lett.* **14**, 4158 (2014).
- <sup>19</sup>X. Wen, A. Ho-Baillie, S. Huang, R. Sheng, S. Chen, H.-C. Ko, and M. A. Green, *Nano Lett.* **15**, 4644 (2015).
- <sup>20</sup>S. Ye, W. Sun, Y. Li, W. Yan, H. Peng, Z. Bian, Z. Liu, and C. Huang, *Nano Lett.* **15**, 3723 (2015).
- <sup>21</sup>A. Yella, L.-P. Heiniger, P. Gao, M. K. Nazeeruddin, and M. Grätzel, *Nano Lett.* **14**, 2591 (2014).
- <sup>22</sup>W. Zhang, M. Anaya, G. Lozano, M. E. Calvo, M. B. Johnston, H. Míguez, and H. J. Snaith, *Nano Lett.* **15**, 1698 (2015).
- <sup>23</sup>G. Hodes, *Science* **342**, 317 (2013).
- <sup>24</sup>H. J. Snaith, *J. Phys. Chem. Lett.* **4**, 3623 (2013).
- <sup>25</sup>S. Y. Sun, T. Salim, N. Mathews, M. Duchamp, C. Boothroyd, G. C. Xing, T. C. Sum, and Y. M. Lam, *Energy Environ. Sci.* **7**, 399 (2014).
- <sup>26</sup>S. D. Stranks, G. E. Eperon, G. Grancini, C. Menelaou, M. J. P. Alcocer, T. Leijtens, L. M. Herz, A. Petrozza, and H. J. Snaith, *Science* **342**, 341 (2013).
- <sup>27</sup>G. C. Xing, N. Mathews, S. Y. Sun, S. S. Lim, Y. M. Lam, M. Gratzel, S. Mhaisalkar, and T. C. Sum, *Science* **342**, 344 (2013).
- <sup>28</sup>S. De Wolf, J. Holovsky, S. J. Moon, P. Loper, B. Niesen, M. Ledinsky, F. J. Haug, J. H. Yum, and C. Ballif, *J. Phys. Chem. Lett.* **5**, 1035 (2014).
- <sup>29</sup>T. S. Ripolles, K. Nishinaka, Y. Ogomi, Y. Miyata, and S. Hayase, *Sol. Energy Mater. Sol. Cells* **144**, 532 (2016).
- <sup>30</sup>G. E. Eperon, G. M. Paterno, R. J. Sutton, A. Zampetti, A. A. Haghighirad, F. Cacialli, and H. J. Snaith, *J. Mater. Chem. A* **3**, 19688 (2015).
- <sup>31</sup>R. E. Beal, D. J. Slotcavage, T. Leijtens, A. R. Bowring, R. A. Belisle, W. H. Nguyen, G. F. Burkhard, E. T. Hoke, and M. D. McGehee, *J. Phys. Chem. Lett.* **7**, 746 (2016).
- <sup>32</sup>M. Kulbak, D. Cahen, and G. Hodes, *J. Phys. Chem. Lett.* **6**, 2452 (2015).
- <sup>33</sup>L. Protesescu, S. Yakunin, M. I. Bodnarchuk, F. Krieg, R. Caputo, C. H. Hendon, R. X. Yang, A. Walsh, and M. V. Kovalenko, *Nano Lett.* **15**, 3692 (2015).
- <sup>34</sup>S. Dastidar, D. A. Egger, L. Z. Tan, S. B. Cromer, A. D. Dillon, S. Liu, L. Kronik, A. M. Rappe, and A. T. Fafarman, *Nano Lett.* **16**, 3563 (2016).
- <sup>35</sup>A. Swarnkar, A. R. Marshall, E. M. Sanehira, B. D. Chernomordik, D. T. Moore, J. A. Christians, T. Chakrabarti, and J. M. Luther, *Science* **354**, 92 (2016).
- <sup>36</sup>R. T. Ross and A. J. Nozik, *J. Appl. Phys.* **53**, 3813 (1982).
- <sup>37</sup>O. D. Mücke and M. Wegener, *Appl. Phys. Lett.* **73**, 569 (1998).
- <sup>38</sup>M. Elsäßer, S. G. Hense, and M. Wegener, *Appl. Phys. Lett.* **70**, 853 (1997).
- <sup>39</sup>M. B. Price, J. Butkus, T. C. Jellicoe, A. Sadhanala, A. Briane, J. E. Halpert, K. Broch, J. M. Hodgkiss, R. H. Friend, and F. Deschler, *Nat. Commun.* **6**, 8420 (2015).
- <sup>40</sup>Y. Yang, D. P. Ostrowski, R. M. France, K. Zhu, J. van de Lagemaat, J. M. Luther, and M. C. Beard, *Nat. Photonics* **10**, 53 (2016).
- <sup>41</sup>H. Kawai, G. Giorgi, A. Marini, and K. Yamashita, *Nano Lett.* **15**, 3103 (2015).
- <sup>42</sup>W. Nie, J.-C. Blancon, A. J. Neukirch, K. Appavoo, H. Tsai, M. Chhowalla, M. A. Alam, M. Y. Sfeir, C. Katan, J. Even, S. Tretiak, J. J. Crochet, G. Gupta, and A. D. Mohite, *Nat. Commun.* **7**, 11574 (2016).
- <sup>43</sup>A. J. Neukirch, W. Nie, J.-C. Blancon, K. Appavoo, H. Tsai, M. Y. Sfeir, C. Katan, L. Pedesseau, J. Even, J. J. Crochet, G. Gupta, A. D. Mohite, and S. Tretiak, *Nano Lett.* **16**, 3809 (2016).
- <sup>44</sup>H. Chung, S. I. Jung, H. J. Kim, W. Cha, E. Sim, D. Kim, W.-K. Koh, and J. Kim, *Angew. Chem., Int. Ed.* **56**, 4160 (2017).
- <sup>45</sup>M. A. Green, *Third Generation Photovoltaics: Advanced Solar Energy Conversion* (Springer-Verlag, Berlin, Heidelberg, 2003).
- <sup>46</sup>D. König, K. Casalenuovo, Y. Takeda, G. Conibeer, J. F. Guillemoles, R. Patterson, L. M. Huang, and M. A. Green, *Physica E* **42**, 2862 (2010).
- <sup>47</sup>J. Shah, *Ultrafast Spectroscopy of Semiconductors and Semiconductor Nanostructures* (Springer-Verlag, Berlin, Heidelberg, 1999), p. 11.
- <sup>48</sup>C. C. Stoumpos and M. G. Kanatzidis, *Acc. Chem. Res.* **48**, 2791 (2015).
- <sup>49</sup>A. Marroonier, H. Lee, B. Geffroy, J. Even, Y. Bonnassieux, and G. Roma, *J. Phys. Chem. Lett.* **8**, 2659 (2017).
- <sup>50</sup>M. Fu, P. Tamarat, H. Huang, J. Even, A. L. Rogach, and B. Lounis, *Nano Lett.* **17**, 2895 (2017).